VOLUME 79 SEPARATE No. 185

PROCEEDINGS

AMERICAN SOCIETY
OF
CIVIL ENGINEERS

APRIL, 1953

NONELASTIC BEHAVIOR OF BRIDGES UNDER IMPULSIVE LOADS

By S. J. Fraenkel and L. E. Grinter, M. ASCE

ENGINEERING MECHANICS DIVISION

Headquarters of the Society
33 W. 39th St.
New York 18, N.Y.

PRICE $0.50 PER COPY

GUIDEPOST FOR TECHNICAL READERS

"Proceedings-Separates" of value or significance to readers in various fields are here listed, for convenience, in terms of the Society's Technical Divisions. Where there seems to be an overlapping of interest between Divisions, the same Separate number may appear under more than one item. For a description of papers open to discussion refer to the current issue of *Civil Engineering*.

Technical Division	*Proceedings-Separate Number*
Air Transport	108, 121, 130, 148, 163, 172, 173, 174, 181, 187 (Discussion: D-75, D-93, D-101, D-102, D-103, D-108, D-121)
City Planning	151, 152, 154, 164, 167, 171, 172, 174, 177 (Discussion: D-65, D-86, D-93, D-99, D-101, D-105, D-108, D-115, D-117)
Construction	160, 161, 162, 164, 165, 166, 167, 168, 181, 183, 184, (Discussion: D-75, D-92, D-101, D-102, D-109, D-113, D-115, D-121, D-126, D-128, D-136)
Engineering Mechanics	145, 157, 158, 160, 161, 162, 169, 177, 179, 183, 185, 186, (Discussion: D-24, D-33, D-34, D-49, D-54, D-61, D-96, D-100, D-122, D-125, D-126, D-127, D-128, D-135, D-136)
Highway	144, 147, 148, 150, 152, 155, 163, 164, 166, 168, 185 (Discussion: D-103, D-105, D-108, D-109, D-113, D-115, D-117, D-121, D-123, D-128)
Hydraulics	154, 159, 164, 169, 175, 178, 180, 181, 184, 186, 187 (Discussion: D-90, D-91, D-92, D-96, D-102, D-113, D-115, D-122, D-123, D-135)
Irrigation and Drainage	148, 153, 154, 156, 159, 160, 161, 162, 164, 169, 175, 178, 180, 184, 186, 187 (Discussion: D-102, D-109, D-117, D-135)
Power	130, 133, 134, 135, 139, 141, 142, 143, 146, 148, 153, 154, 159, 160, 161, 162, 164, 169, 175, 178, 180, 184, 186 (Discussion: D-96, D-102, D-109, D-112, D-117, D-135)
Sanitary Engineering	55, 56, 87, 91, 96, 106, 111, 118, 130, 133, 134, 135, 139, 141, 149, 153, 166, 167, 175, 176, 180, 187 (Discussion: D-97, D-99, D-102, D-112, D-117, D-135)
Soil Mechanics and Foundations	43, 44, 48, 94, 102, 103, 106, 108, 109, 115, 130, 152, 155, 157, 166, 177 (Discussion: D-86, D-103, D-108, D-109, D-115)
Structural	145, 146, 147, 150, 155, 157, 158, 160, 161, 162, 163, 164, 165, 166, 168, 170, 175, 177, 179, 181, 182, 183, 185, 188 (Discussion: D-51, D-53, D-54, D-59, D-61, D-66, D-72, D-77, D-100, D-101, D-103, D-109, D-121, D-125 D-126, D-127, D-128, D-136)
Surveying and Mapping	50, 52, 55, 60, 63, 65, 68, 121, 138, 151, 152, 172, 173 (Discussion: D-60, D-65)
Waterways	123, 130, 135, 148, 154, 159, 165, 166, 167, 169, 181 (Discussion: D-19, D-27, D-28, D-56, D-70, D-71, D-78, D-79, D-80, D-112, D-113, D-115, D-123, D-135)

A constant effort is made to supply technical material to Society members, over the entire range of possible interest. Insofar as your specialty may be covered inadequately in the foregoing list, this fact is a gage of the need for your help toward improvement. Those who are planning papers for submission to "Proceedings-Separates" will expedite Division and Committee action measurably by first studying the ASCE "Guide for Development of Proceedings-Separates" as to style, content, and format. For a copy of this pamphlet, address the Manager, Technical Publications, ASCE, 33 W. 39th Street, New York 18, N. Y.

Published at Prince and Lemon Streets, Lancaster, Pa., by the American Society of Civil Engineers. Editorial and General Offices at 33 West Thirty-ninth Street, New York 18, N. Y. Reprints from this publication may be made on condition that the full title of paper, name of author, page reference, and date of publication by the Society are given.

Proceedings—Vol. 79 April, 1953 Separate No. 185

AMERICAN SOCIETY OF CIVIL ENGINEERS
Founded November 5, 1852

PAPERS

NONELASTIC BEHAVIOR OF BRIDGES UNDER IMPULSIVE LOADS

By S. J. Fraenkel[1] and L. E. Grinter,[2] M. ASCE

Synopsis

A method for predicting the effects of loads that vary with time on bridges and other structures when deformations extend into the plastic range is presented in this paper. Although such analyses are necessarily more complex than the use of statics, the method presented requires only numerical techniques. Hence, the computations are of a routine nature fitted to the procedures of a design office. The bridge studies reported in this paper aid in determining which bridges, under atomic attack, are most susceptible to damage, and the bridge characteristics that are desirable for resisting blast.

Because the immediate questions would be whether the span should be long or short, whether mass is to be added or avoided, whether girders or trusses are to be preferred, and what effect is to be expected from change of elevation above the water, the answers to these questions were sought. In order to reduce the number of variables, a group of simple railway spans ranging from 50 ft to 519 ft were studied to determine the permanent deflections produced by the explosion of a nominal atomic bomb 2,000 ft vertically above the center of the span. The numerical answers obtained are not as significant, of course, as the relative damage sustained as a function of span, mass, elevation, and type of structure.

Preliminary Considerations

The determination of dynamic effects on bridges is not new since much has been written about impact loadings on bridge spans and related phenomena. However, the problem of blast damage differs in two important aspects from previous work in this field. Former studies have been concerned with dynamic

Note.—Written comments are invited for publication; the last discussion should be submitted by October 1, 1953.

[1] Asst. Chairman, Structural Research Dept., Armour Research Foundation of Illinois Inst. of Tech., Chicago, Ill.

[2] Dean, Graduate School, and Director of Research, Univ. of Florida, Gainesville, Fla.

forces originating from wheel unbalance that produces a periodic forcing function traveling along the span, whereas the concern in this study is a nonperiodic uniformly distributed loading, which is a function of time. The methods proposed do not limit the variation of the load with time as long as this variation can be expressed mathematically or graphically.

The second departure from conventional engineering considerations lies in the emphasis which is placed on the nonelastic behavior of the bridge. In determining the amount of damage that a given bridge may suffer as a result of an explosion, only the plastic range of behavior is of interest. Moreover, the changing configuration of the bridge, after the forces have deformed it beyond the elastic limit, must be established.

The principal simplification available for the study of configuration follows from the common assumption of plasticity that yielding of a single member of a statically determinate truss transforms the structure into a mechanism. Irrespective of the questions that may be raised as to the influence of gussets, rivet holes, welds, continuity of chords, and other structural details, present design practice assumes that any properly designed truss or girder span must deflect well into the plastic range before fracture occurs because brittle fracture is not comtemplated in standard specifications. Hence, analysis based on the mechanism concept is believed to be a satisfactory method of evaluating the relative influence of a parameter, such as length of span, on the resistance to deflection from atomic blast for bridges that are essentially similar. Once this concept of transformation of the structure into a mechanism consisting of two rigid bodies joined by a plastic member is accepted, the motion of each body may be studied by the equations of dynamic equilibrium. Such equations can be solved by numerical stage-by-stage analysis using an appropriate interval of time between successive stages.

The structures selected as examples for study are simple-span trusses and girders of a single-track railway type. The uniform impulsive loading chosen is that produced by an atomic explosion of a 20-kiloton bomb (equivalent to 20,000 tons of trinitrotoluene (TNT) at 2,000 ft directly above the span. The method of analysis developed could be adjusted, with only moderate complication, to handle nonuniform loading and statically indeterminate spans such as suspension bridges, continuous girders, and rigid frame bridges. An impulsive load of any type may be handled as long as the pressure-time variation is completely known. The character of the differential equations that describe the motion of the bridge does not encourage the hope that a closed solution may be obtained, and it seems likely that numerical methods will continue to be required for the solution of the equations. The amount of labor involved in carrying through a stage-by-stage analysis of the type suggested is well within reason, however.

Definition of Damage.—Reference has already been made to relative damage as a measure of the resistance of a bridge to atomic blast. For quantitative comparisons it is necessary to define structural damage in numerical terms despite the realization that the degree of damage assigned to any structure after a balst will be dependent on such factors as the difference between wartime and peace, the importance of the structure to a given operation, the possi-

bility of control over traffic, the visibility of the damage, and other similar factors. In this paper, the ratio of the maximum nonrecoverable deflection to the span length is taken as a quantitative index of structural damage. This index is related to such physical factors as the slope of the floor, the change in the critical internal angle of the truss triangle, and the external angle that develops between the two rigid bodies joined by the plastic member.

The ratio of deflection to span is readily determined, and it seems to be a reasonable criterion of structural damage, considering the symmetrical uniform loading and the expressed intention to study large nonelastic movements. It might properly be suggested that a better index of damage would be, for example, the percentage of actual change of length to the permissible change of length of the plastic member. However, until more is known about the action of built-up tension and compression members in the plastic range so that limits may be assigned to total axial deformations for members of different lengths, cross sections, and end conditions, a simpler index of damage such as the one described, seems preferable. Hence, all procedures of analysis presented herein furnish values of the maximum deflection as the final result.

Development of a Procedure of Analysis

The analytical processes comprise the determination of the loading acting on the bridge; the movement within the elastic range, resulting in the maximum elastic deflection; and the movement within the plastic range which produces nonrecoverable deflection.

Determination of Loads.—The first step in computing the loads acting on the bridge requires consideration of some of the basic phenomena surrounding the explosion of an atomic bomb. Such an explosion creates pressures in the atmosphere—varying with both time and distance from the point of explosion—which can be described roughly as shock waves expanding spherically around the source. The pressure difference existing between the undisturbed air in front of the shock wave and the air behind it is called the "over-pressure," which decreases gradually to zero. The variation (with time) of free air pressure at a point is given by the expression:[3]

$$p_s = (P_s)_{max} \left(1 - \frac{t}{t_0}\right) e^{-t/t_0} \qquad (1)$$

in which p_s equals the over-pressure in shock wave at the time t; $(P_s)_{max}$ is equal to the peak over-pressure (often termed "side-on" pressure); t represents time, measured from the beginning of the positive phase; and t_0 denotes the duration of the positive phase of the blast wave.

It also can be determined that, at a distance of 2,000 ft from an exploding nominal bomb, the peak over-pressure is 24 lb per sq in., which decreases to zero in a period of 0.45 sec, according to the upper curve[4] in Fig. 1. Thus, it is possible to determine the over-pressure existing at any time during the positive phase for the particular case of interest.

[3] "The Effects of Atomic Weapons," Govt. Printing Office, Washington, D. C., 1950, p. 124.
[4] *Ibid.*, p. 135.

For bridge locations displaced laterally from beneath the point of explosion of the bomb, the "Mach stem" will produce an essentially horizontal side-on shock to the bridge.[5,6] The intensification of the pressure in the Mach stem and the small lateral resistance in some bridges may cause greater vulnerability to such loadings than to the vertical loadings considered herein. This vulnerability can be determined only by a study of the methods to be discussed.

However, knowledge of the variation of over-pressure with time at the location of the bridge is not sufficient for determining vertical loads. The loading on the bridge depends largely on the geometry of the bridge itself because the pressures and their variation with time during the action of the shock wave on the bridge are functions of the size and shape of the structure. When the shock front first arrives at the bridge floor, it increases immediately to the "reflected pressure" which is two or more times the original over-pressure. This excess pressure then flows around the edges of the object struck in order to equalize itself with the surrounding over-pressures; this process is referred to

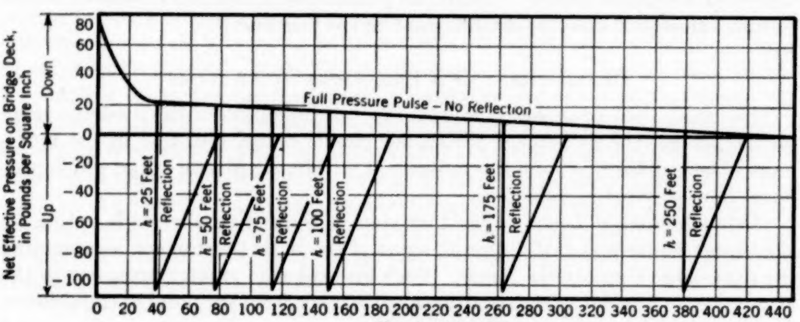

FIG. 1.—PRESSURE-TIME CURVE FOR 519-FT BRIDGE

as "diffraction" and is dependent on the size and shape of the object struck by the shock front. Considering the simple rectangular shape of a bridge structure viewed from above, and the predominant contribution made by the solid deck of the bridge to the total area struck by the wave, the structure will be idealized to that of a flat plate (corresponding to the deck) that is struck by a shock wave. It is important to recall that it is the expressed objective to determine relative nonelastic deflections for several bridges and that approximations having a comparable effect on all structures may be accepted. With this simplification, results from shock tube experiments may be used to determine the pressure distribution as a function of time during the diffraction process. A shock tube is a pipe in which pressure can be built up and then suddenly released, causing a shock wave to travel down the tube. The data used actually were obtained for a thin plate fixed at the bottom of the shock tube and struck normally by a passing shock wave of intensity comparable to an over-pressure of 24 lb per sq in. The results are derived from interfero-

[5] "The Effects of Atomic Weapons," Govt. Printing Office, Washington, D. C., 1950, p. 67.
[6] *Ibid.*, p. 76.

metric measurements and are in terms of dimensionless pressure ratios expressed as functions of time.[7] For reasons of symmetry the thin plate used in shock tube studies is considered to represent the half-width of the bridge deck. It is suggested that, in studies of this kind, the flat plate that simulates the bridge deck in the shock tube be considered to represent the width of the bridge between the outboard edges of the chords, rather than that of the deck proper, in order to compensate, as far as is practicable, for the neglect of the resistance to the vertical shock of the individual truss members.

The diffraction period is followed by a relatively long period of drag that is caused by the flow of air away from the explosion during the positive phase. Shock tube data are limited, for practical reasons, to the initial diffraction period, but it can be shown that conventional drag formulas give values of pressures that agree well with the end values of the shock tube information. It seems permissible, therefore, to extend the pressure-time curve based on shock tube results with a straight line passing through zero pressure at the end of the positive phase. A typical curve of this kind is shown in Fig. 1, in which it is designated as "Full Pressure Pulse—No Reflection."

The loading phenomena previously described are those which would be expected to occur if the bridge where located by itself in an infinite atmosphere, or were so far removed from other obstructions to the shock wave that it would not be affected by their presence. Actually, this is not likely to be the case except where the elevation of the span above the ground or water surface is unusually great. It becomes necessary, therefore, to consider the effects of elevation of the span above the surface of the earth, and it will be shown that the reflection of the shock wave from the ground or water beneath the bridge will alter the loading considerably.

It is helpful to draw first a qualitative picture of the successive phenomena in the reflection process. First, the original shock wave impinges on the top side of the bridge floor and is diffracted around it. The shock wave is reformed underneath the bridge and impinges on the ground or water surface below, whereupon it is reflected with intensified strength and travels upward into a "once-shocked" region. The mass flow behind the returning shock wave is zero—that is, the air is at rest. The reflected shock wave impinges on the bottom surface of the bridge floor, exerting upward pressure on it. The reflected shock wave is then diffracted around the deck and travels farther upward, after reforming above the deck. Following this, no further air forces act on the bridge.

A quantitative treatment of this procedure will not be given in this paper because it would require far too much space. However in the performance of other investigations of this kind it should be kept in mind that both water and earth, being of high acoustic impedance relative to air, reflect shock without appreciable loss of energy and that, until further experimental data become available, the upward diffraction process must be approximated from the same shock tube data as the initial downward diffraction. Also, because of the presence of a turbulent region immediately beneath the deck, the strength of the

[7] "The Diffraction of Shock Waves around Obstacles and the Resultant Transient Loading of Structures," by D. R. White, D. K. Weimer, and W. Bleakney, *Technical Report II-6*, Princeton Univ., Princeton, N. J., August 1, 1950.

returning shock wave, reflected from the earth's surface below, should be reduced by one third when the reflected pressure on the underside of the deck is computed. Attention must be paid to the fact that the returning shock wave enters a region in which the over-pressure is continuously decreasing. Assuming the latter to remain constant is probably permissible for elevations up to about 100 ft with a shock of 24 lb per sq in., but this assumption will introduce serious error for greater heights or stronger shocks.

The pressure-time relations that are obtained for various elevations of a 510-ft span are shown in Fig. 1, in which the bridge deck elevation is expressed as h. It is apparent that the case of no reflection differs radically in its pressure-time relationship from the case of reflection from any commonly encountered height. The time required for the reflected shock to make itself felt increases with increasing elevation of the bridge, and the upward impulse furnished by the reflection becomes a progressively smaller percentage of the downward impulse as the elevation increases. The large upward forces exerted by the reflected shock waves may account for the phenomenon observed in Hiroshima and Nagasaki, in Japan, where even those bridges close to "ground zero" suffered little structural damage. Unfortunately, evidence on this point is very meager.[8]

Present knowledge of the actual loading is surrounded by many uncertainties. An analytical treatment of this problem seems virtually impossible, and only fragmentary experimental data applicable to diffraction around complex structures have been published. Therefore, the numerical results obtained from such data are open to question as to their accuracy, although it should be kept in mind that in this study accuracy of loading is secondary to the establishment of general relations between bridge characteristics and damage. The validity of such comparisons is not influenced by the accuracy of the loading information to as great an extent as are individual numerical answers.

Motion in the Elastic Range.—The initial motion of the bridge under the applied load is in the elastic range. The theoretical response to a suddenly applied load is the excitation of the various elastic modes of the bridge. Because consideration is restricted herein to uniform loading on a symmetrical bridge, there is no need for the inclusion of even harmonics that correspond to unsymmetrical deflection profiles. The treatment may be simplified further by assuming the elastic response configuration to be the static deflection profile or, essentially, by using the first mode of vibration. Since experimental evidence justifies this assumption for the case of a concentrated central dynamic load, it seems certain that a uniformly distributed load would follow the static deflection profile even more closely.[9]

It is desirable, as a matter of convenience, to reduce the problem of determining the center deflection as a function of time to that of determining the motion-time history of a lumped single-degree-of-freedom system. The motion of such a system may be treated with Duhamel's integral, although other methods are also possible. Considering the nonmathematical character of the

[8] "The Effects of Atomic Weapons," Govt. Printing Office, Washington, D. C., 1950, p. 152.

[9] "Investigation of Bridge Impacts with a Mechanical Oscillator," *Bulletin*, Am. Ry. Eng. Assn., 1948, p. 61.

forcing function—that is, the pressure variation with time—it is desirable to express the integral in incremental form for tabular integration,[10,11] as follows:

$$y_1 = y_0 \cos \omega \Delta + \frac{\dot{y}_0}{\omega} \sin \omega \Delta + \frac{F}{m\,\omega^2}(1 - \cos \omega \Delta) \qquad \text{(2a)}$$

and

$$\frac{\dot{y}_1}{\omega} = -\,y_0 \sin \omega \Delta + \frac{\dot{y}_0}{\omega} \cos \omega \Delta + \frac{F}{m\,\omega^2} \sin \omega \Delta \qquad \text{(2b)}$$

in which y is equal to the center deflection, in feet; $\dot{y}$ equals the center velocity, in feet per second (the dot notation for time derivatives is used here and throughout this paper); F represents the total applied load, in pounds; m equals the mass of the entire bridge, in pound-feet per second per second; ω is equal to the natural frequency of the bridge in the fundamental mode, in cycles per second; Δ denotes the time interval, in seconds; and the subscripts 0 and 1 correspond to deflections at any two consecutive instants.

The equivalent linear oscillator should not only possess the same natural frequency as the bridge, but it also should undergo the same static deflections. If the entire mass of the bridge is used as the mass m of the oscillator, and if the natural frequencies of the bridge and the oscillator are equal, then the oscillator will have an excessive stiffness k. Consequently, a fictitious driving force must be used for equal static deflections of the bridge and the oscillator model, which is obtained by multiplying the actual forcing function by the ratio of the stiffness of the oscillator to that of the bridge. The adjustment can also be made by using a suitably reduced mass and retaining the actual forcing function.

The integration of Eqs. 2a and 2b requires that the natural frequency of the bridge and its limiting elastic deflection be computed. The following relations are available for the determination of these frequencies:

For truss railway bridges, in which δ_{st} is the dead load deflection in inches,

$$\frac{\omega}{2\pi} = f = \frac{12}{\sqrt{\delta_{st}}} \qquad \text{(3)}$$

in which f is the natural frequency, in cycles per second; and for girder railway bridges,

$$f = \frac{12.4}{\sqrt{\delta_{st}}} \qquad \text{(4)}$$

Variations of the moment of inertia along the span need not be considered and the center value may be used in the determination[12] of δ_{st}.

The determination of the limiting elastic deflection is necessary in order to terminate the stage-by-stage integration of Eqs. 2a and 2b when the deflection passes from the elastic into the plastic region. Eqs. 2a and 2b do not apply beyond this point, of course. The computation of the limiting elastic deflection is simple in principle, although rather laborious, and is illustrated through the description of the various steps involved for a truss bridge, as follows:

---

[10] "Advanced Dynamics," by S. Timoshenko and D. H. Young, McGraw-Hill Book Co., Inc., New York, N. Y., 1948, p. 54.

[11] *Ibid.*, p. 311.

[12] "A Mathematical Treatise on Vibrations in Railway Bridges," by Sir Charles E. Inglis, Cambridge University Press, Cambridge, England, 1934, p. 11.

1. The dead load stresses in each member are determined.

2. The capacity of each member, which may be taken as the yield stress times the effective cross-sectional area, is determined, with allowance for buckling in compression members.[13]

3. The remaining capacity of each member is computed by subtracting the dead load stress from the computed capacity.

4. The live load stress in each member is determined for a uniformly distributed live load.

5. The deflection produced at the center by the live load is computed from step 4.

6. By proportion, the uniformly distributed live load that will exhaust the remaining capacity (as obtained in step 3) is computed for the most highly stressed member.

7. The deflection caused by the live load obtained in step 6 is computed. This deflection is the limiting elastic deflection.

The integration of Eqs. 2*a* and 2*b* for the elastic range can be illustrated readily by the numerical example in the Appendix.

Motion in the Plastic Range.—The terminal values for the elastic range, obtained as explained in the Appendix, furnish the limiting elastic deflection, the time at which this deflection is reached, and the downward velocity of the bridge at that time. These terminal values of the elastic case constitute the initial conditions for the plastic range.

The basic treatment of the plastic case is based on the consideration that yielding in a single member in a statically determinate structure (or of the last redundant member plus one in an indeterminate system) converts the structure into a mechanism. The equations of motion for constrained rigid bodies may be used to follow the ensuing motion in the plastic range. Hence, for the statically determinate truss, it is assumed that only one plastic member exists and that the members that remain elastic form essentially rigid links in a kinematic chain. Actually, these links are elastic and will be vibrating elastically. Their individual elastic displacements, however, are so small in relation to the sum of the elastic and plastic displacements of the entire span that they will be neglected. Also, when dealing with bridges with solid deck floors, it appears satisfactory for purposes of comparison to assume the trusses to be equivalent to bars in the plane of the floor. Where greater numerical accuracy is desired, the actual mass distribution of the truss can be taken intc account readily in the computations.

It seems reasonable to make the assumption that a condition of "perfect plasticity" exists—that is, no account will be taken of possible strain hardening. This assumption is justified for strains less than from ten to twenty times the elastic strains in structural steels, as is confirmed by the stress-strain diagram and the tests of actual laboratory structures. Beyond the range of deformation the structure develops added resistance by virtue of strain hardening that will be neglected in the computations. Other simplifying assumptions include the neglect of strain-rate and multi-axial effects, the omission of secondary stress, the

[13] "Design of Modern Steel Structures," by L. E. Grinter, The Macmillan Co., New York, N. Y., 1941, p. 185, Fig. 97.

convention of frictionless joints in trusses, and the convenient use of a total plastic cross section when the yield point is reached in the extreme fiber of girder sections. It is believed that none of these approximations affect the validity of the results significantly, at least as far as comparative computed damage for generally similar structures is concerned.

The equations of motion in the plastic range are derived for a girder bridge, a truss bridge with flow occurring in the top chord, and a truss bridge with flow occurring in the bottom chord. The equations have been derived in the general form and then have been simplified successively in each case for small angles of rotation and also for a symmetrical deflection configuration. In the case of girder bridges symmetry exists. However, even a symmetrical bridge no longer can be considered as such when inertia forces are involved because one end of the span is pinned whereas the other is free to slide, so that the bridge becomes, in effect, a slider-crank type of mechanism. The complete derivation of the equations would require too much space to be included herein; instead,

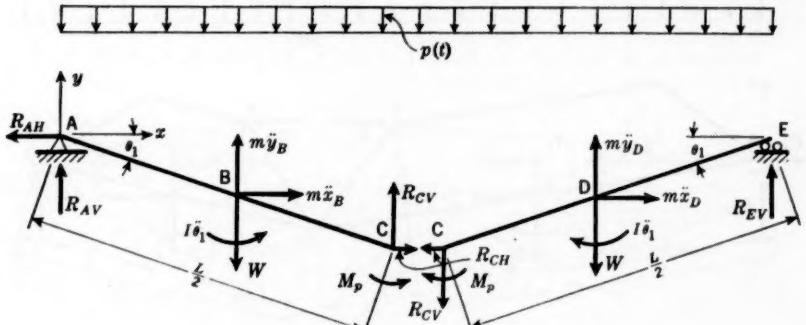

FIG. 2.—GEOMETRY OF GIRDER IN PLASTIC RANGE

the derivation of a simple case will be given in outline form and the equations for all other cases will be written in final form.

Equations of Motion for a Girder Bridge.—The equation of motion for any rigid link, such as is shown in the left-hand part of Fig. 2, may be written by an equation of dynamic equilibrium which makes use of the inertia forces $m\,\ddot{y}_B$, $m\,\ddot{x}_B$, and $I_B\,\ddot{\theta}_1$; the loads, p, W; and the reactions at both ends of the link. The symbol x indicates horizontal displacement, the symbol I denotes the mass moment of inertia about the point indicated by the subscript, and W is the dead load over one half of the span. A convenient expression is obtained from the equation $\Sigma\,M_A = 0$ for the forces of Fig. 2, in which M is a moment about the point indicated by the subscript. It will be recalled that the moment of the three inertia terms about A is equivalent to $I_A\,\ddot{\theta}_1$ in which the subscript 1 refers to the left half of the bridge. Hence,

$$\Sigma\,M_A = 0 = \tfrac{1}{8}\,p\,L^2\cos^2\theta_1 + \tfrac{1}{4}\,W\,L\cos\theta_1 - M_p - R_{CH}\left(\frac{L}{2}\sin\theta\right) - R_{CV}\left(\frac{L}{2}\cos\theta\right) - I_A\,\ddot{\theta}_1.$$

Transferring the inertia moment to the opposite side of the equation and expressing R_{CV} and R_{CH} from their values obtained from the equations, $\Sigma F_x = 0$ and $\Sigma F_y = 0$, applied to Fig. 2,

$$I_A \ddot{\theta}_1 = \tfrac{1}{8} p L^2 \cos^2 \theta_1 - M_p + \tfrac{1}{4} m L^2 \sin \theta_1 (\cos \theta_1 \dot{\theta}^2_1 + \sin \theta_1 \ddot{\theta}_1) + \tfrac{1}{4} W L \cos \theta_1 \quad (5)$$

The equation for small angles of rotation, θ, is

$$I_A \ddot{\theta}_1 - 3 I_A \theta_1 \dot{\theta}^2_1 = \tfrac{1}{8} p L^2 - M_p + \tfrac{1}{4} W L \quad (6)$$

in which I_A denotes the mass moment of inertia of the left half of the bridge about point A; θ_1, $\dot{\theta}_1$, and $\ddot{\theta}_1$ equal angular displacement, velocity, and acceleration about point A, respectively; M_p represents the maximum plastic moment of the girder section; and W denotes the weight of one half of the girder. All other symbols are illustrated in Fig. 2.

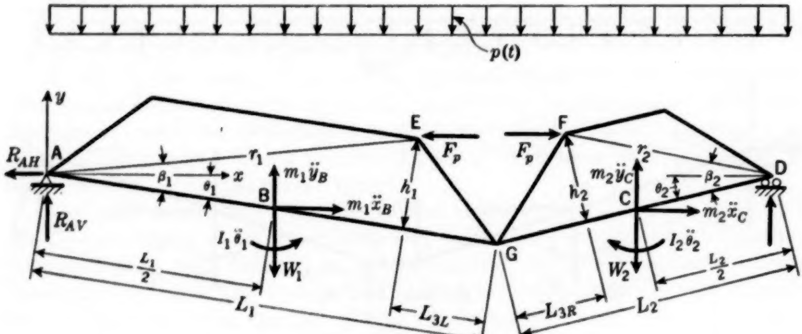

FIG. 3.—GEOMETRY OF TRUSS BRIDGE UNDERGOING FLOW IN A TOP CHORD MEMBER

Truss Bridge with Plastic Flow in Top Chord.—With reference to Fig. 3, the general equation of motion is

$$\begin{aligned} I_A \ddot{\theta}_1 = {} & \tfrac{1}{2} W_1 L_1 \cos \theta_1 + F_p \sin \alpha \, (h \sin \theta_1 + r_1 \cos \beta_1 \cos \theta_1) \\ & - F_p \cos \alpha \, (h \cos \theta_1 - r_1 \cos \beta_1 \sin \theta_1) + \tfrac{1}{2} p L^2_1 \cos^2 \theta_1 \\ & + R_{GV} L_1 \cos \theta_1 - R_{GH} L_1 \sin \theta_1 \quad (7) \end{aligned}$$

in which I_A equal the mass moment of inertia of the left part of the bridge about point A; W_1 is equal to the weight of the left part of bridge; F_p represents the force in the plastic member; $\alpha = \tan^{-1} \dfrac{(y_F - y_E)}{(x_F - x_E)}$;

$$\begin{aligned} R_{GC} = {} & - \tfrac{1}{2} p (L_1 \cos \theta_1 - L_2 \cos \theta_2) - (W_1 - m_1 \ddot{y}_B) \frac{\tfrac{1}{2} L_1 \cos \theta_1}{L_1 \cos \theta_1 + L_2 \cos \theta_2} \\ & - F_p \sin \alpha + \frac{I_1 \ddot{\theta}_1 - I_2 \ddot{\theta}_2}{L_1 \cos \theta_1 + L_2 \cos \theta_2} + \frac{1}{L_1 \cos \theta_1 + L_2 \cos \theta_2} \\ & \times [(m_1 \ddot{x}_B + m_2 \ddot{x}_C) \tfrac{1}{2} L_1 \sin \theta_1 - (m_2 \ddot{y}_C - W_2) \tfrac{1}{2} L_2 \cos \theta_2]; \end{aligned}$$

and

$$R_{GH} = m_2 \ddot{x}_C + F_p \cos \alpha.$$

The equation for small angles of rotation, θ, is

$$\left[\tfrac{1}{3} m_1 L^2{}_1 \left(1 - \frac{L_1}{L_1 + L_2}\right) + \tfrac{1}{3} \frac{L_1}{L_1 + L_2} m_2 L_1 L_2\right] \ddot{\theta}_1 - \left[m_2 \frac{L_1}{L_1 + L_2} (L^2{}_1 + L_1 L_2)\right] \theta_1 \dot{\theta}^2{}_1 = \tfrac{1}{2} W_1 L_1 \left(1 - \frac{L_1}{L_1 + L_2}\right) + \tfrac{1}{2} W_2 L_2 \frac{L_1}{L_1 + L_2} - F_p (h + L_{3L} \theta_1) - F_p \alpha L_{3L} + \tfrac{1}{2} p L_1 L_2 \quad (8)$$

The equation for small angles of rotation, θ, and for the symmetrical mode of yielding is

$$\tfrac{1}{3} m_1 L^2{}_1 \ddot{\theta}_1 - m_1 L^2{}_1 \theta_1 \dot{\theta}^2{}_1 = \tfrac{1}{2} W_1 L_1 - F_p (L_{3L} \theta_1 + h) + \tfrac{1}{2} p L^2{}_1 \quad (9)$$

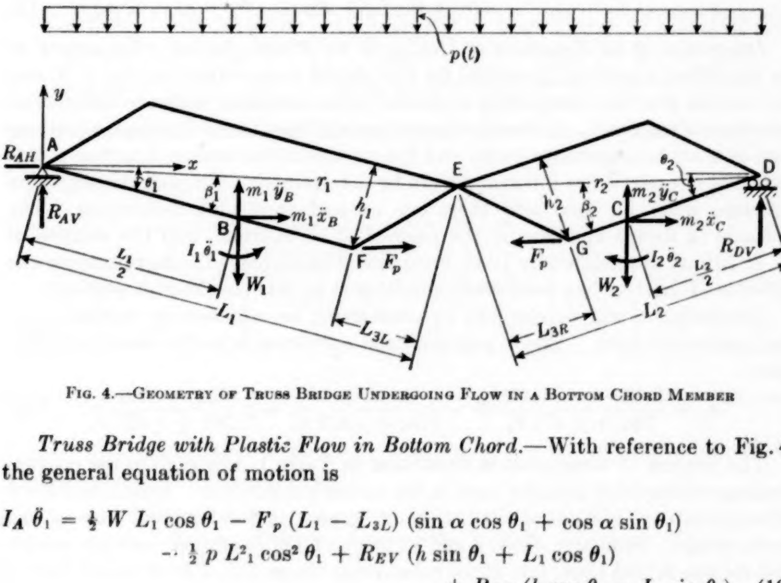

FIG. 4.—GEOMETRY OF TRUSS BRIDGE UNDERGOING FLOW IN A BOTTOM CHORD MEMBER

Truss Bridge with Plastic Flow in Bottom Chord.—With reference to Fig. 4, the general equation of motion is

$$I_A \ddot{\theta}_1 = \tfrac{1}{2} W L_1 \cos \theta_1 - F_p (L_1 - L_{3L}) (\sin \alpha \cos \theta_1 + \cos \alpha \sin \theta_1) - \tfrac{1}{2} p L^2{}_1 \cos^2 \theta_1 + R_{EV} (h \sin \theta_1 + L_1 \cos \theta_1) + R_{EH} (h \cos \theta_1 - L_1 \sin \theta_1) \quad (10)$$

in which $\alpha = \tan^{-1} \dfrac{(y_G - y_F)}{(x_G - x_F)}$;

$$R_{EV} = -\tfrac{1}{2} p (L_1 \cos \theta_1 - L_2 \cos \theta_2) - (W_1 - m_1 \ddot{y}_B) \frac{\tfrac{1}{2} L_1 \cos \theta_1}{L_1 \cos \theta_1 + L_2 \cos \theta_2} + F_p \sin \alpha + \frac{I_1 \ddot{\theta}_1 - I_2 \ddot{\theta}_2}{L_1 \cos \theta_1 + L_2 \cos \theta_2} + \frac{1}{L_1 \cos \theta_1 + L_2 \cos \theta_2} \times [(m_1 \ddot{x}_B + m_2 \ddot{x}_C) \tfrac{1}{2} L_1 \sin \theta_1 - (m_2 \ddot{y}_C - W_2)' \tfrac{1}{2} L_2 \cos \theta_2)];$$

and

$$R_{EH} = m_2 \ddot{x}_C - F_p \cos \alpha.$$

The equation for small angles of rotation, θ, is

$$\left[\tfrac{1}{3} m_1 L^2{}_1 + \frac{L_1}{L_1 + L_2} (\tfrac{1}{6} m_1 L^2{}_1 - \tfrac{1}{6} m_2 L_1 L_2) + m_2 \frac{2 L_1 L_2 + L^2{}_1}{2 L_2} h \theta_1\right] \ddot{\theta}_1$$
$$+ \left[m_2 \theta_1 \left(\frac{L^3{}_1 + L^4{}_1/L_2}{2 (L_1 + L_2)} - L^2{}_1 - \frac{L^3{}_1}{2 L_2}\right) + m_2 h \left(L_1 + \frac{L^2{}_1}{2 L_2}\right)\right] \dot{\theta}^2{}_1$$
$$= \tfrac{1}{2} W_1 L_1 \left(1 - \frac{L_1}{L_1 + L_2}\right) + \tfrac{1}{2} W_2 L_2 \frac{L_1}{L_1 + L_2}$$
$$- \tfrac{1}{2} p \left[(L_1 - L_2) h \theta_1 - L_1 L_2\right] - F_p (h - L_{3L} \theta_1) + F_p \alpha L_{3L} \quad \text{..(11)}$$

The equation for small angles of rotation, θ, and for the symmetrical mode of yielding is

$$(\tfrac{1}{3} m_1 L^2{}_1 + \tfrac{3}{2} m_1 L_1 h \theta_1) \ddot{\theta}_1 - m_1 L_1 (L_1 \theta_1 - \tfrac{3}{2} h) \dot{\theta}^2{}_1$$
$$= \tfrac{1}{2} W_1 L_1 + F_p (L_{3L} \theta_1 - h) + \tfrac{1}{2} p L^2{}_1 \quad \text{..(12)}$$

Integration of the Equations of Motion for the Plastic Region.—Inspection of the simplified equations of motion for the plastic range—that is, Eqs. 6, 9, and 12—reveals that the integration of second-order nonlinear ordinary differential equations is required. A closed solution has not been found for these equations even in their homogeneous form, and the nature of the forcing function $p(t)$ is such that the particular integral cannot be determined. Numerical integration therefore must be used and there are several applicable techinques. The methods of Runge and Kutta, the method of C. Störmer, and the method of W. E. Milne, as modified by L. R. Ford, could be employed. In this paper the last-named method has been used, adapting it to this problem as required.

The problem will be clarified by considering an equation of motion in its final numerical form. The example chosen corresponds to the case of a 519-ft span:

$$\ddot{\theta}_1 = \frac{3{,}405\, \theta_1 - 1{,}471}{764 + 1{,}471\, \theta_1} \dot{\theta}^2 - \frac{279}{764 + 1{,}471\, \theta_1} + p \frac{258 + 17.5\, \theta_1}{764 + 1{,}471\, \theta_1} \quad \text{....(13)}$$

The process of integration is illustrated in Table 1, which gives the column headings of the table actually used in the numerical solution. Cols. 1 and 2 are self-explanatory, the initial time, t, being chosen as the terminal time of the elastic range. Similarly, Cols. 3 and 12 can be filled in at once from the elastic case for the initial time, but at all subsequent times Col. 3 is obtained from a Taylor expansion, as follows:

$$\theta\Big|_{t_1 = t_0 + \Delta} = \theta\Big|_{t = t_0} + \frac{\Delta}{2} \dot{\theta}\Big|_{t = t_0} + \frac{1}{2}\left(\frac{\Delta}{2}\right)^2 \ddot{\theta}\Big|_{t = t_0} \quad \text{..........(14)}$$

in which Δ is the time interval selected. Col. 12 requires a similar prediction of $\dot{\theta}$; hence,

$$\dot{\theta}\Big|_{t_1 = t_0 + \Delta} = \dot{\theta}\Big|_{t = t_0} + \frac{\Delta}{2} \ddot{\theta}\Big|_{t = t_0} \quad \text{................(15)}$$

Values for θ_0 and $\dot{\theta}_0$ thus having been established for Cols. 3 and 12, respectively, it is possible to complete all columns up to and including Col. 14. According to the equation itself, the algebraic addition of Cols. 10, 11, and 14 gives a value for $\ddot{\theta}_0$, shown in Col. 15. It becomes necessary to obtain an improved value of

TABLE 1.—TABULAR SOLUTION OF EQ. 13

Time, t (sec) (1)	Pressure, p (lb per sq in.) (2)	Angular displacement, θ_0 (radians) (3)	$1{,}471\ \theta_0$ (4)	$17.5\ \theta_0$ (5)	$3{,}405\ \theta_0$ (6)	$764 + 1{,}471\ \theta_0$ (7)

$258 + 17.5\ \theta_0$ (8)	$1{,}470 - 3{,}405\ \theta_0$ (9)	$p\dfrac{258 + 17.5\ \theta_0}{764 + 1{,}471\ \theta_0}$ (10)	$\dfrac{279}{764 + 1{,}471\ \theta_0}$ (11)	Angular velocity, $\dot{\theta}_0$ (radians per sec) (12)

$\dot{\theta}^2_0$ (13)	$\dfrac{1{,}470 - 3{,}405\ \theta_0}{764 + 1{,}471\ \theta_0}\cdot\dot{\theta}^2_0$ (14)	Angular acceleration, $\ddot{\theta}_0$ (radians per sec per sec) (15)	$\dot{\theta}_1$ (radians per sec) (16)	θ_1 (radians) (17)	$\ddot{\theta}_1$ (radians per sec per sec) (18)	$\dot{\theta}_2$ (radians per sec) (19)	θ_2 (radians) (20)

θ_0 and of $\dot{\theta}_0$ (designated θ_1 and $\dot{\theta}_1$, respectively) for the next iteration cycle. The particular formulas used are[14]

$$\left.\begin{aligned} \dot{\theta}\Big|_{t=t+2\Delta} &= \dot{\theta}_t + \frac{\Delta}{3}\left[\ddot{\theta}_t + 4\ddot{\theta}\Big|_{t+\Delta} + \ddot{\theta}\Big|_{t+2\Delta}\right] \\ \theta\Big|_{t=t+2\Delta} &= \theta_t + \frac{\Delta}{3}\left[\dot{\theta}_t + 4\,\dot{\theta}\Big|_{t+\Delta} + \dot{\theta}\Big|_{t+2\Delta}\right] \end{aligned}\right\} \qquad (16)$$

A slight variation of these formulas is desirable for the initial interval Δ in order to obtain greater accuracy in the beginning. By using Eqs. 16 it is possible to complete Cols. 16 and 17. At this point a new cycle of iteration begins and the procedure repeats itself since the values of $\dot{\theta}_1$ and θ_1 in Cols. 16 and 17 are analogous to $\dot{\theta}_0$ and θ_0 given in Cols. 12 and 3. The results of the next cycle

[14] "Differential Equations," by L. R. Ford, McGraw-Hill Book Co., Inc., New York, N. Y., 1933, p. 159.

are given in Cols. 18, 19, and 20. Column headings for the second iteration cycle are not shown in Table 1 because Cols. 4 to 14 would simply repeat themselves, with all subscripts changed from 0 to 1, and from 1 to 2.

Actual numerical solutions are not presented because of the voluminous character of the computations. It was found that agreement between θ_2 in Col.

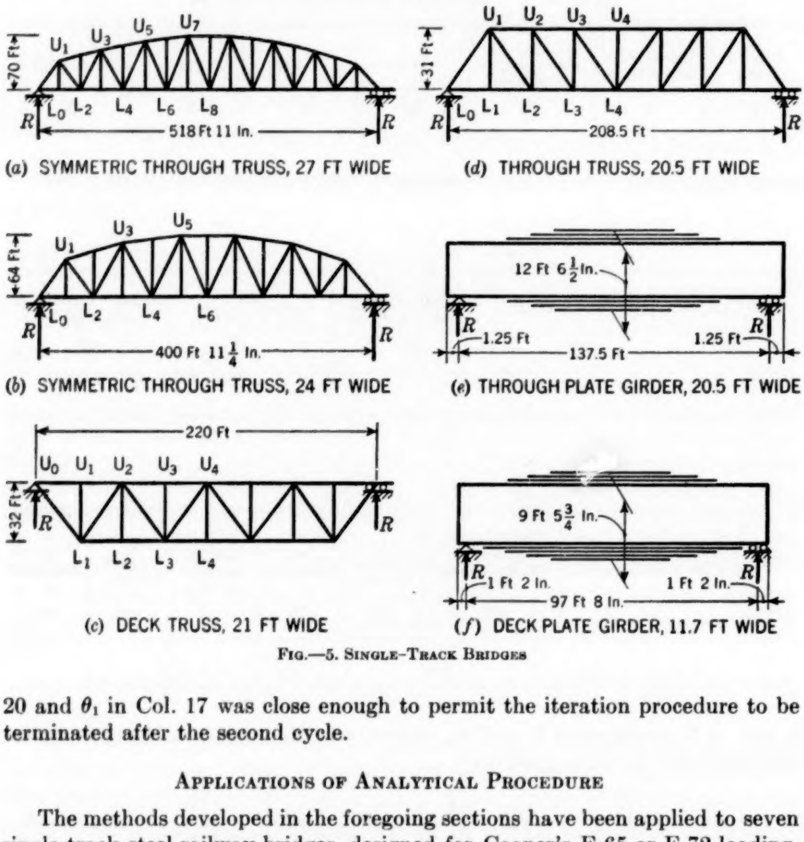

Fig.—5. Single-Track Bridges

20 and θ_1 in Col. 17 was close enough to permit the iteration procedure to be terminated after the second cycle.

Applications of Analytical Procedure

The methods developed in the foregoing sections have been applied to seven single-track steel railway bridges, designed for Cooper's E-65 or E-72 loading, and supported by pins at one end and by rollers at the other. All, except the 140-ft girder span, have solid deck floors of standard weight, and all are statically determinate. The specific structures investigated are those shown in Figs. 5 and a 50-ft rolled-beam bridge, which is not shown. The particular variables investigated were the effect of span length on resistance to impulsive loading resulting from an atomic explosion 2,000 ft above the bridge, the difference between deck and through construction with respect to such resistance, and the effect of elevations between 50 ft and 175 ft above ground or water surface (for the 519-ft bridge) on the damage from such an explosion.

Presentation of Results

The immediate result obtained from a "plastodynamic" analysis is the value of the center or maximum deflection of the bridge as a function of time. The time at which the plastic deformation terminates may be inherent in the loading and the resistance of the structure or plastic flow may continue virtually

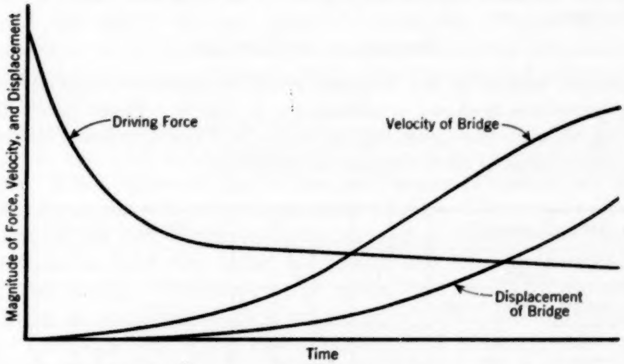

Fig. 6.—Driving Force and Bridge Response Variation with Time

indefinitely. However, deformation that is greater than a certain limiting range of values is of little interest. For example, if it is assumed, that a ratio of maximum deflection to a span length of 5% corresponds to total uselessness or collapse of the bridge, it is unimportant to determine how much larger the

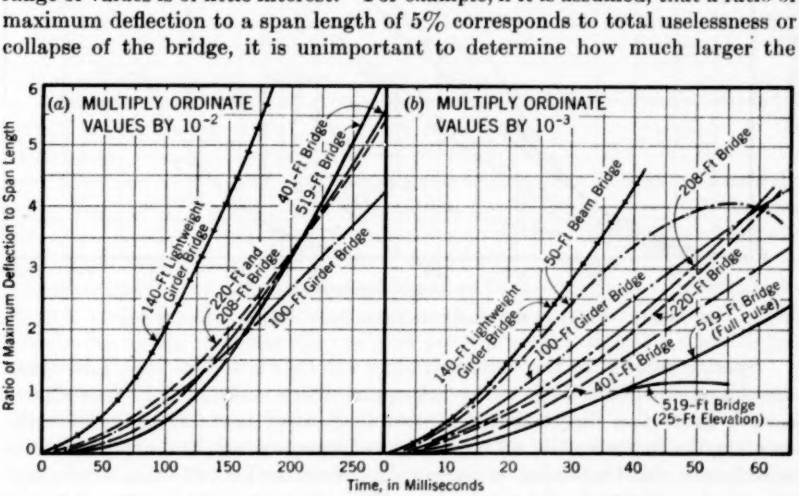

Fig. 7.—Variation with Time of the Ratio of Maximum Deflection to Span Length

deflection could grow. This assumption makes possible the use of the equations for small angles of rotation which represent a vast simplification of the general case. It must be further understood that the equations presented apply only while the angular velocity $\dot{\theta}$ remains positive because the reverse motion implies

elastic behavior of the structure rather than constant resistance to deformation. In any event, the procedure may be terminated when the physically significant limit of the deflection, of the deflection-span ratio, or of any other selected criterion of damage is judged to have been reached. This limit depends on the particular structure. For example, it seems reasonable to assume that the limiting value for highway bridges would be significantly higher than that for railway bridges.

Discussion of Results

The general nature of the displacement-time relations determined by the foregoing procedure is shown qualitatively in Fig. 6. These curves illustrate the time lag between the increasing deflection and the decreasing driving force, and they are typical of all the spans investigated.

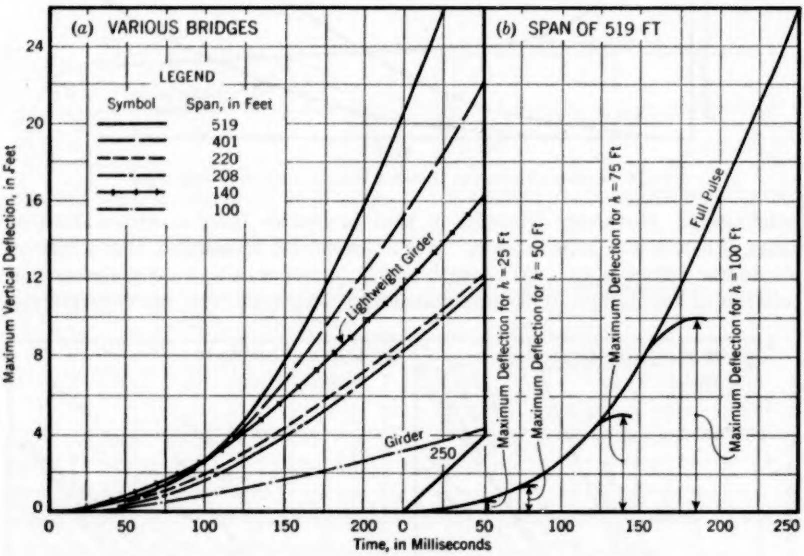

Fig. 8.—Relation Between Time and Maximum Vertical Deflection

Specific results for the various bridges are shown in Fig. 7(*a*). All spans are shown except the 50-ft rolled-beam span which was omitted for reasons of scale. From this illustration it is seen that, after approximately 250 milliseconds, the deflections of all the bridges of standard weight increase with the span length, and that the given pulse will produce the highest ratio of deflection to span length for the longest bridge. The situation is reversed in the early stages, as is shown more clearly in Fig. 7(*b*), because the greater inertia of the longer spans delays the development of speed and displacement. Thus, it can be seen that ultimate damage should increase with increasing span. The 140-ft girder span forms a rather remarkable exception to this pattern, and its behavior has been attributed to its lightweight construction and unusually large

deck area. The curve for the 140-ft span indicates that a reduction of mass may lead to very undesirable consequences in bridges acted upon by pressure pulses of this type. It is not possible to isolate completely the effect of mass variation by means of the results shown, however, because no two bridges studied differed in mass only.

It may be noted also that the difference in behavior between the 220-ft deck bridge and the 208-ft through bridge is negligible. Therefore, it may be accepted that deck and through bridges have approximately the same resistance to blast and that no reason exists (on the basis of the present evidence) to favor one over the other.

The variation with time of the deflection-span ratio is shown to an expanded time scale in Fig. 7(*b*), so that the initial phases of the motion become distinguishable. It is clearly seen that, in the early stages of motion, the deflection-span ratio increases with decreasing span length. The motion of the 50-ft span is illustrated, and it is noticed that its motion remains elastic throughout. This result agrees with the earlier conclusion that damage increases with increasing span length. The lower curve in Fig. 7(*b*) illustrates the effect of reflection from an elevation of 25 ft on the 519-ft span and shows graphically that this bridge, which is the most vulnerable of all the spans, would not even enter the plastic range if it were located within 25 ft of the ground or of the water surface.

The relations represented in Fig. 8(*a*) are essentially similar to those shown in Fig. 7 but give the actual deflection in feet as a function of time. Again, the maximum deflection increases with span length, except for the lightweight, unballasted 140-ft span which shows deflections that might be expected of a 300-ft span of standard ballasted construction.

The remarkable effects of elevation above the surface are illustrated for the 519-ft bridge in Fig. 8(*b*). The short segments of curves correspond to the motions for the heights shown, whereas the full curve coincides with that shown in Fig. 8(*a*) for this span. It is apparent that, for elevations substantially exceeding 100 ft, the downward deflection of the bridge is so great by the time the upward pulse arrives that the latter has no significantly helpful effect, and the bridge must be presumed to have been rendered useless. It is obvious, on the other hand, that, for elevations of less than 75 ft, the effects of reflection are drastic and that this effect may save such a span from destruction. This conclusion agrees with the observations made after the Hiroshima and Nagasaki bombings.

By studying Fig. 7 some interesting conclusions may be drawn regarding the maximum height above ground for which an important inhibiting effect is exerted on the damage to spans of various lengths. The curves in Fig. 7 show that, after about 220 milliseconds, a given ratio of maximum deflection to span length is reached at a later time for shorter spans. Considering a certain ratio of permanent deflection to span, or a specified extent of damage, more time can be allowed for the return of the shock wave for short spans because the length of time required to produce this extent of damage is greater for short spans. Therefore, the benefit derived from the returning shock wave may be obtained during a longer period of time while the bridge is being deformed. This longer

time corresponds to the reflection period for an increased elevation above the ground or water surface. Thus, it can be concluded that the maximum elevation, for which reflection has an important inhibiting effect on damage, increases with decreasing span length.

One further observation should be made which does not refer directly to the aforementioned illustrations. A comparison of the differential equations of motion for girder and truss bridges, Eqs. 6 and 12, show that the "resistance" term is $-M_p$ for the girder and $-F_p(h - L_{3L}\theta_1)$ for the truss. Assuming that a girder and a truss bridge of equal span weigh the same, when designed for the same loading, the inertia and weight terms need be of no concern in this comparison. If the deck area is also the same for the two bridges, the same driving force will be exerted, and the resulting nonelastic deflection will depend inversely and approximately on the resistance terms. However, it will be noted that the magnitude of the resistance term for the girder is constant, M_p, but that of the truss bridge decreases with increasing rotation θ_1. Thus, it may be presumed that a truss bridge will suffer greater permanent deflection and damage than a girder bridge, provided both are of the same weight and span and are designed according to the same specifications. Unfortunately, it is not possible to include such a pair of comparable examples herein, and the results obtained do not permit isolation of the effect of span length from that of truss or girder construction. On the other hand, the extreme reduction of deflection from the 208-ft truss bridge to the 100-ft girder bridge, shown in Fig. 8(*a*), does not appear wholly attributable to a reduction in the span alone. Therefore, it may be concluded that the numerical results are not inconsistent with the presumption that there is a significant difference between the inelastic behavior of truss and girder bridges.

Summary and Conclusions

This paper has proposed a method for the determination of deflections produced by impulsive vertical loadings on simple-span bridges of truss and girder types. These procedures cover both elastic and large nonelastic deflections, and their use involves only moderate expenditures of time and technical effort. The method can be extended to treat statically indeterminate structures.

The development of the procedures involves the use of several physical assumptions, which are discussed in the body of the paper. The two most important assumptions are the equivalence of a plastically deformed bridge to a mechanism involving rigid and plastic parts, and the feasibility of extrapolating transient shock loading data obtained from small shock tube models to full-size structures. The numerical solution of the differential equations of motion is essentially exact from the engineering viewpoint for both the elastic and the plastic ranges.

The procedures suggested have been applied to the case of an impulsive loading produced by the explosion of a nominal atomic bomb at 2,000 ft above the bridge. Simple-span truss and girder bridges of steel ranging from 50 ft to 519 ft in length were investigated. Since incomplete information on the validity of the underlying assumptions should not vitiate conclusions based

on comparisons between the computed response of different bridges of the same general type, the results obtained are believed to justify the following specific conclusions:

1. Damage from nonelastic vertical deflection produced by an atomic blast, measured either directly or as a percentage of span length, increases with increasing span.
2. Damage increases with increasing width of bridge—all other things remaining equal.
3. Damage to two bridges of the same span and differing only in weight should be greater for the bridge having the smaller weight.
4. Height of a bridge above ground or water influences markedly the damage sustained. A bridge that may be destroyed in the absence of shock wave reflection from the ground may suffer no damage at all if it is sufficiently close to the ground or water surface.
5. In the case of the 519-ft bridge, computations show that the maximum elevation above ground for which a significant benefit is derived from reflection is about 100 ft. At greater heights, the returning shock wave arrives too late to prevent the bridge from being rendered useless.
6. It has been found that the maximum elevation above ground for which the reflected shock wave will have an important inhibiting effect on damage will increase with decreasing length of the bridge.
7. The elastic and nonelastic behaviors of deck bridges and through truss bridges are essentially alike under an overhead atomic blast, and there appears to be no reason to prefer one or the other from this aspect.
8. If a truss bridge and a grider bridge have the same weight and span, and if they are designed under the same specifications, it may be reasoned from mathematical considerations that blast damage of the girder bridge should be less than that of the truss bridge.

APPENDIX. NUMERICAL EXAMPLE

The equations of motion for the elastic range (Eqs. 2) take the following form for the 519-ft through truss bridge:

$$y_1 = 0.9992\, y_0 + 0.0389 \frac{\dot{y}_0}{9.73} + 0.001334\, p \quad \text{(17a)}$$

and

$$\frac{\dot{y}_1}{9.73} = -\,0.0389\, y_0 + 0.9992 \frac{\dot{y}_0}{9.73} + 0.00685\, p \quad \text{(17b)}$$

(Subscripts 0 and 1 refer to consecutive values of y and $\dot{y}$ with respect to time.) The tabular solution then proceeds as shown in Table 2, in which the first three lines of the integration process are given. Col. 1 gives the time, at intervals of four milliseconds. The corresponding values of the pressure are then read from the pressure-time curve in Fig. 1. Cols. 3 and 4 then follow, and values of zero may be entered for Cols. 5 and 8 in the first line because the bridge is

presumed to be initially at rest. The deflection y after $t = 0.004$ sec, in the second line, may be obtained from Eq. 17*a*, as follows:

$$y\Big|_{t=0.004} = 0.9992\, y\Big|_{t=0} + 0.0389\,\frac{\dot{y}|_{t=0}}{9.73} + 0.0001334\, p\Big|_{t=0.004}$$
$$= 0 + 0 + 0.00846 = 0.00846.$$

TABLE 2.—SOLUTION OF EQS. 17

Time, t (sec)	Pressure, p (lb per sq in.)	$0.00685\,p$ (lb per sq in.)	$0.0001334\,p$ (lb per sq in.)	Deflection, y (ft)	$0.9992\,y$ (ft)	$0.0389\,y$ (ft)	$\frac{\dot{y}}{9.73}$ (ft per sec)	$0.9992\,\frac{\dot{y}}{9.73}$ (ft)	$0.0389\,\frac{\dot{y}}{9.73}$ (ft)
(1)	(2)	(3)	(4)	(5)	(6)	(7)	(8)	(9)	(10)
0	75	0.514	0.01001	0			0		
0.004	63.5	0.435	0.00846	0.00846	0.00845	0.00033	0.435	0.435	0.015
0.008	54	0.369	0.00720	0.03065	0.03065	0.00119	0.804	0.804	0.0313

Cols. 6 and 7 then follow by direct multiplication. The second equation is used to obtain $\dot{y}$:

$$\frac{\dot{y}|_{t=0.004}}{9.73} = -0.0389\, y\Big|_{t=0} + 0.9992\,\frac{\dot{y}|_{t=0}}{9.73} + 0.00685\, p\Big|_{t=0.004}$$
$$= 0 + 0 + 0.435 = 0.435,$$

which is shown in Col. 8. Cols. 9 and 10 follow directly. For the next line, in which $t = 0.008$—

$$y\Big|_{t=0.008} = 0.9992\, y\Big|_{t=0.004} + 0.0389\,\frac{\dot{y}}{9.73}\Big|_{t=0.004} + 0.0001334\, p\Big|_{t=0.008}$$

or, the values in Col. 5, line 3, are obtained by adding together the values in Col. 6, line 2; Col. 10, line 2; and Col. 4, line 3. Thus, $y\Big|_{t=0.008} = 0.03065$. Similarly, $\frac{\dot{y}}{9.73}\Big|_{t=0.008} = 0.804$, obtained by adding algebraically the following values: Col. 7, line 2; Col. 9, line 2; and Col. 3, line 3. This procedure continues in this manner until y reaches the limiting elastic deflection beyond which it is no longer applicable.

CURRENT PAPERS

Proceedings-Separate Number	Title and Author	Discussion closes*
159	"Development of a Flood-Control Plan for Houston, Tex.," by Ellsworth I. Davis	June 1
160	"Ice Pressure Against Dams: Studies of the Effects of Temperature Variations," by Bertil Löfquist	June 1
161	"Ice Pressure Against Dams: Some Investigations in Canada," by A. D. Hogg	June 1
162	"Ice Pressure Against Dams: Experimental Investigations by the Bureau of Reclamation," by G. E. Monfore	June 1
163	"A Comparison of Design Methods for Airfield Pavements," Progress Report of the Committee on Correlation of Runway Design Procedures of the Air Transport Division	June 1
164	"Water Supply Engineering," Report of Committee on Water Supply Engineering of the Sanitary Engineering Division for the Period Ending September 30, 1951	July 1
165	"Design Curves for Anchored Steel Sheet Piling," by Walter C. Boyer and Henry M. Lummis, III	July 1
166	"The Design of Flexible Bulkheads," by James R. Ayers and R. C. Stokes	July 1
167	"Sewage Disposal in Tidal Estuaries," by Alexander N. Diachishin, Seth G. Hess, and William T. Ingram	July 1
168	"Special Design Features of the Yorktown Bridge," Maurice N. Quade	July 1
169	"Rating Curves for Flow over Drum Gates," by Joseph N. Bradley	Aug. 1
170	"Rapid Computation of Flexural Constants," by Thomas G. Morrison	Aug. 1
171	"Unified Mass-Transportation System for New York," by William Reid	Aug. 1
172	"Aeronautical Charting and Mapping," by Charles A. Schanck	Aug. 1
173	"Electronic Devices for Air Transport," by F. B. Lee	Aug. 1
174	"Zoning Maps for Airports," by Benjamin Everett Beavin, Sr.	Aug. 1
175	"Design of Side Walls in Chutes and Spillways," by D. B. Gumensky	Aug. 1
176	"Advances in Sewage Treatment and Present Status of the Art," Progress Report of the Committee of the Sanitary Engineering Division on Sewerage and Sewage Treatment	Sept. 1
177	"Earthquake Stresses in Shear Buildings," by M. G. Salvadori	Sept. 1
178	"Rainfall Studies Using Rain-Gage Networks and Radar," by H. E. Hudson, Jr., G. E. Stout, and F. A. Huff	Sept. 1
179	"Stiffness Charts for Gusseted Members Under Axial Load," by John E. Goldberg	Sept. 1
180	"A Direct Step Method for Computing Water-Surface Profiles," by Arthur A. Ezra	Sept. 1
181	"Slackwater Improvement of the Columbia River," by O. E. Walsh	Oct. 1
182	"Hipped Plate Analysis, Considering Joint Displacement," by Ibrahim Gaafar	Oct. 1
183	"Group Loadings Applied to the Analysis of Frames, by I. F. Morrison	Oct. 1
184	"Dam Modifications Checked by Hydraulic Models," by E. S. Harrison and Carl E. Kindsvater	Oct. 1
185	"Nonelastic Behavior of Bridges Under Impulsive Loads," by S. J. Fraenkel and L. E. Grinter	Oct. 1
186	"Settling Rates of Suspensions in Solids Contact Units," by A. A. Kalinske	Oct. 1
187	"The Equivalent Rectangle in Prestressed Concrete Design," by John J. Peebles	Oct. 1
188	"Laminar to Turbulent Flow in a Wide Open Channel," by W. M. Owen	Oct. 1

* Readers are urged to submit discussion applying to current papers. Forty free Separates per year are allotted to members. Mail the coupon order form found in the current issue of *Civil Engineering.*